An experimental study of the dilation factor in sandstone under anisotropic stress conditions

Arpita Pal-Bathija and Mike Batzle, Colorado School of Mines*

SUMMARY

Dilation factor (R) is defined as the ratio of relative change in velocity to relative change in deformation. R has significant implications for time-lapse(4D) seismic studies where it can be used to infer reservoir compaction or overburden expansion from seismic changes.
In situ stresses are usually unequal in the vertical and horizontal directions. And these anisotropic stress conditions are a dominant factor controlling acoustic velocities and strain. We conducted deformation and ultrasonic experiments to study the effect of triaxial stress on dilation factor. Two different sandstone samples with different porosities were used in the experiments. Measured absolute R values ranged from 6 to 91.
R values are dependent on the deformation mechanisms causing the strain. Dynamic Young's modulus (low amplitude) is generally higher than the static Young's modulus (high amplitude) as they correspond to different deformation mechanisms. Hence, theoretical models that use the same mechanisms to describe both wave propagation and macroscopic deformation are not valid. The ratio of dynamic to static moduli depends on the direction of stress applied with respect to the density and placement of compliant pores.
R values were also found to be strongly dependent on the stress states, hence using a constant value of R from the seafloor to the reservoir depth should be avoided. Reduced stress sensitivity of velocities at higher confining pressures led to lower absolute values for R. R values are different for P and S waves, especially in the presence of fluids.

INTRODUCTION

Detecting geomechanical changes to predict well failure and to monitor reservoir depletion opens up new ways of using 4D data. Time-lapse seismic monitoring of pressure-induced changes in depleting North Sea gas fields reveals that detectable differences in seismic arrival times are observed above the reservoir interval (Hatchell et al., 2003).

Forward models of time-lapse time shifts are constructed from stress and strain fields computed using geomechanical models and a stress-strain-dependent seismic velocity (Hatchell and Bourne, 2005b). Based on observations of time-lapse seismic data from several locations around the world, they found that a simple linear model relating seismic velocity with vertical normal strain works well in all cases. Time shifts are computed as the product of vertical normal strain and velocity-strain coupling coefficient(-R). Their observations also show that the velocity-strain dependence is larger for rock elongation than for rock contraction. The former is about 5 and the latter is less than half this value. They obtained theoretical estimates of -R values in the range of 1-3 from empirical velocity-porosity trends and in the range of 2-10 using crack models.

Various investigations have documented the change in velocities with stress. However, the sample deformations occurring during these measurements are rarely reported. This study will significantly contribute to understand the inconsistencies in the R values. We conducted ultrasonic experiments and static deformation measurements to study the effect of triaxial stress on the dilation factor in sandstone.

DATA

The experimental equipment consisted of a confining pressure vessel, an axial stress controller, a pressure pump and transfer vessel for controlling pore pressure, a digital oscilloscope, a pulse generator, and ultrasonic transducers attached at the top, bottom and sides of the sample, a data acquisition device and a computer. Resistive strain gages were used to measure deformation.

Cylindrical samples were subjected to radial stress (confining pressure) and axial stress. The bedding plane was normal to the axial direction for Berea sandstone with porosity of 19%. No visible bedding plane symmetry was observed in the Foxhills sandstone sample with porosity of 24%. For Berea, only the velocities and strain parallel to the uniaxial stress direction were measured, whereas for Foxhill, the velocities and strain parallel and normal to the uniaxial stress direction were measured.

Hydrostatic data were measured when the axial and radial stresses were equal. Uniaxial stress measurements were made while increasing axial stress at various constant radial stresses. The axial and radial shear waves were both polarized radially. Figure 1 shows the measurement space over which the data were collected for each sample.

Note that this is a more general acquisition method and allow analyses along arbitrary stress paths as compared to most studies which collect data only along specific stress paths. The effect of saturation was studied by comparing dry and brine-saturated samples. Data in this study correspond to the downloading cycle of confining pressure to simulate the reservoir conditions under production.

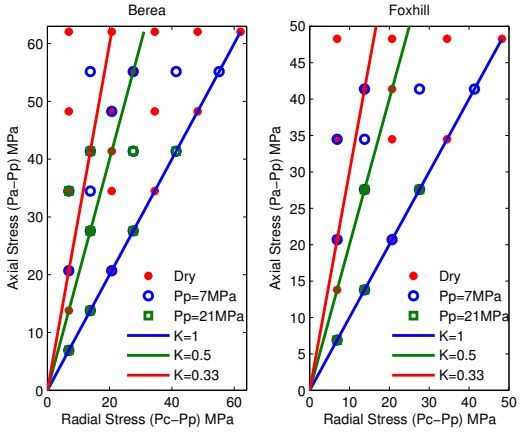

Figure 1: Measurement states. Each point represents a location in stress space where velocities were measured. Deformation in the sample was continuously recorded throughout the experiment. K refers to a constant ratio of radial stress to axial stress. The hydrostatic line (K=1) is for equal stresses. Lithostatic lines with K = 0.5 and K = 0.33 are also shown.

The strain values were calibrated by shunting the calibration resistor across an active strain gage arm of the same resistance, as used on the samples. The values matched well with documented data. The velocities and Young's moduli values were calibrated with measurements on an aluminum sample.

We define "cracks" as compliant pores, which can be described as hav-

ing lower aspect ratio. Aspect ratio is the ratio of minor to the major axis of an elliptical pore. Thus, thin open pore spaces between distributed grain boundaries are also referred as cracks in this study.

The dilation factor (R) was calculated by finding the ratio of the change in velocity over initial velocity to strain (Equation 1),

$$R = \frac{\frac{\Delta V}{V}}{\varepsilon} \tag{1}$$

where V is velocity and ε is strain in the direction of velocity measurement. Strain is the dimensionless ratio of change in length with respect to original length $\left[\frac{\Delta L}{L}\right]$ and is considered to be negative for compression/compaction and positive for tension/elongation in this study. R value is negative as velocity decrease is associated with sample elongation or velocity increase with compaction.

Static Young's modulus was obtained from uniaxial stress data, where the axial stress was increased at constant radial stresses. Young's modulus, E_s, is the slope of the stress strain curve as shown in Equation 2,

$$E_s = \frac{d\sigma_{zz}}{d\varepsilon_{zz}} \tag{2}$$

where $d\sigma_{zz}$ is the incremental uniaxial stress and $d\varepsilon_{zz}$ is the strain change along the same zz direction as the uniaxial stress. In our study, $d\sigma_{zz}$ refers to $[P_a - P_c]$ and $d\varepsilon_{zz}$ refers to $\left[\varepsilon_{\parallel P_a > P_c} - \varepsilon_{\parallel P_a = P_c}\right]$ where, P_c is confining pressure and P_a is axial stress.

Dynamic Young's modulus was computed using Equation 3,

$$E_d = \frac{\rho V_s^2 \left[3V_p^2 - 4V_s^2\right]}{V_p^2 - V_s^2} \tag{3}$$

where ρ is the density of the rock and V_p, V_s are the compressional and shear velocities. In our study, V_p, V_s refer to $V_{p\parallel}$, $V_{s\parallel}$ respectively, as those are parallel to the uniaxial stress direction.

Relative uncertainty involved in hand-picking first arrival travel times was found to be ± 0.01. The relative uncertainty in strain was calculated to be ± 0.005. The relative uncertainty in dilation factor (R) was the same as the relative uncertainty in strain, since the uncertainties in the velocities compensate each other (Equation 1). The error bars are contained in the size of the symbols for R. Note that these are measurement uncertainties, and does not include systematic errors or biases such as sample heterogeneity, bad gage mounting etc.

RESULTS

Static vs. Dynamic

Static (macroscopic and isothermal) elastic moduli are equal or lower than the dynamic (adiabatic) moduli (Simmons and Brace, 1965; Jizba et al., 1990; Zimmer, 2003; Olsen and Fabricius, 2006). The difference between static and dynamic moduli is related more to the amplitude of the measurement than to the frequency. Very low amplitude P and S waves are not expected to cause motion or frictional sliding along grain boundaries and therefore only sense open pore space compliance.

An increase in stiffness due to decrease in porosity (Berea vs. Foxhill) is evident from Figure 2. Increasing stiffness at higher confining pressures is also seen in both the samples in Figure 2 due to the closure of cracks. With uniaxial stress increment, the ratio of dynamic to static Young's modulus remains constant for Berea, whereas for Foxhill, this ratio increases. The modulus ratio remains almost constant for Berea, as it initially had more high aspect ratio pores than Foxhill. Increase of uniaxial stress in Foxhill generates more open cracks owing to the higher density of cracks parallel to the uniaxial stress direction.

Since the static and dynamic Young's moduli are different for both the sandstone samples, the static strains will be different from dynamic strains. Hence, the R values are dependent on the deformation mechanism used to cause the strain. In time-lapse seismic data, the velocities correspond to the dynamic mechanism, while strain is inferred from static mechanisms, such as sea floor subsidence and reservoir compaction (Hatchell and Bourne, 2005a; Rϕste et al., 2005). Theoretical models that use rock properties trends, derived from velocity-porosity regression, microcrack model, asperity-deformation model and hertz-mindlin model (Rϕste et al., 2005; Hatchell and Bourne, 2005b) use the same dynamic mechanism to calculate the change in velocities as well as strains. Hence comparing those modeled R values with the 4D seismic data is inconsistent.

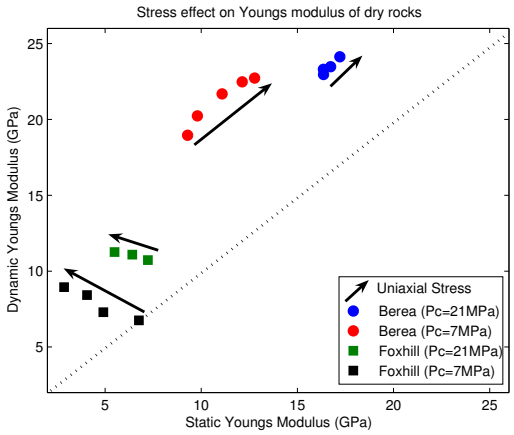

Figure 2: Static versus Dynamic Young's modulus. Increasing stiffness with lower porosity and higher confining pressure (Pc) is evident. The ratio of dynamic to static Young's modulus remains almost constant for rocks with less cracks (Berea) and increases for cracks oriented parallel to the uniaxial stress direction (Foxhill).

Anisotropy

We used the Thomsen (1986) anisotropy parameters ε and γ, to infer about crack-induced anisotropy. We did not have the data to calculate the important seismic anisotropy parameters δ and η. We see that crack induced anisotropy increases with axial stress, and this increase is more pronounced at lower confined stress states (Figure 3). Sarkar et al. (2003) also demonstrated that the time-lapse changes of anisotropy can provide useful information about temporal variations in the stress field.

Dilation Factor

A hydrostatic stress decrease results in a decrease in all velocities. And the magnitude of this change increases at low pressures due to increased stress sensitivity of the velocity, owing to more open cracks and compliant pores. These cracks and compliant pores result in smaller strains as compared to the change in velocities at low pressures. Hence, the absolute R values are higher at lower pressures (when the change in hydrostatic pressure increases) as seen in Figure 4.

The absolute R values decrease with saturation for P-waves as shown in Figure 5. This is because a fluid makes the rock stiffer as its cavities are filled with less compressible fluid. Hence the change in velocities as compared to strains are much smaller as compared to the dry case. S-wave velocities are less sensitive to fluid saturation as seen in Figure 5. Greater stress sensitivity at lower confining or differential pressures leading to higher absolute R values are also seen in Figure 5.

A uniaxial stress increase results in a decrease in absolute R values of the waves propagating (or being polarized) along the applied stress. The absolute R values of the waves propagating (or being polarized)

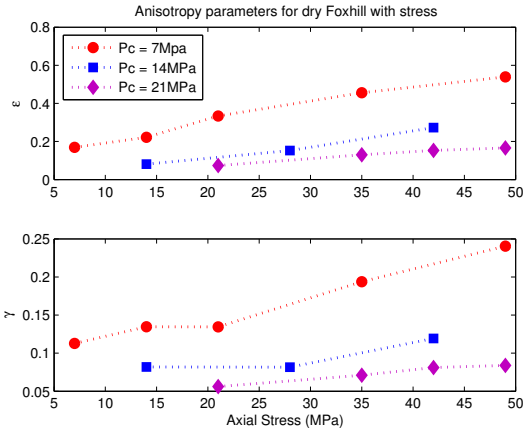

Figure 3: Anisotropy parameters plotted as a function of axial stress. Crack-induced anisotropy increases with axial stress, and this increase is much more at lower confined stress states.

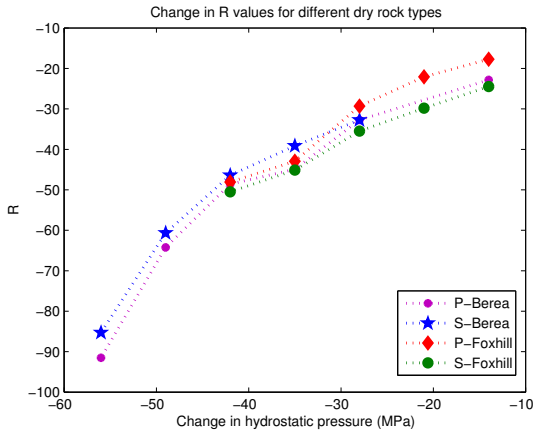

Figure 4: R values are plotted as a function of hydrostatic pressure changes. Note that the greatest change in hydrostatic pressure is at the lowest confining pressure, where absolute R value is the highest.

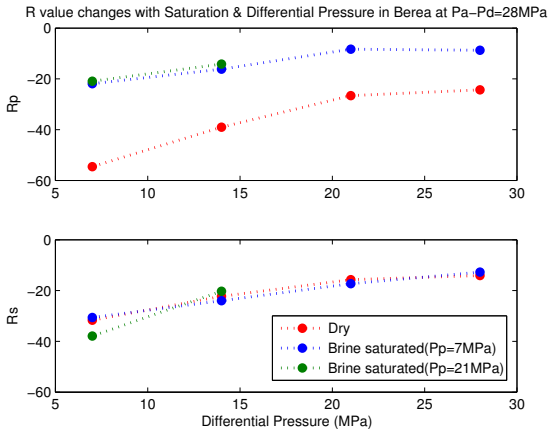

Figure 5: Berea sandstone R value changes with fluid saturation and differential pressure at a constant difference between the axial stress and the differential pressure. Absolute Rp value decreases with fluid saturation and increasing differential pressure. Since Vs in Berea sandstone is relatively insensitive to fluid saturation, Rs is also insensitive to fluid saturation.

normal to this direction are also reducing as seen in Figure 6. This happens because a compressive stress component normal to a crack face may close the crack, thus increasing the velocities in the direction along applied stress. New cracks primarily aligned with the maximum principal stress will be generated or old cracks might open up due to compressive loading if the cracks faces are parallel to the stress direction. The length changes being larger than velocity changes reduce the absolute R values. Figure 7 and Figure 8 show the components of R i.e., change in velocity over initial velocity changes and strain changes with uniaxial stress increments. Holt et al. (2005) also supported this behavior using model calculations.

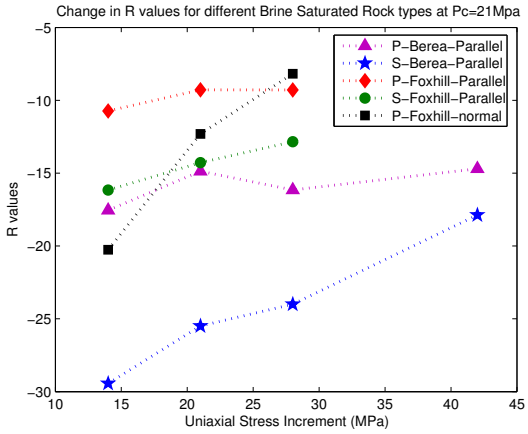

Figure 6: R values are plotted against uniaxial stress increments at a constant differential pressure P_d of 14 MPa ($= 21(P_c) - 7(P_p)$). Parallel and normal are with respect to the uniaxial stress direction. Notice the crack-induced anisotropy in the R values for Foxhill.

DISCUSSION

Hydrocarbon depletion and fluid injection in the reservoirs cause compaction and stretching of the reservoir and overburden layers. R values

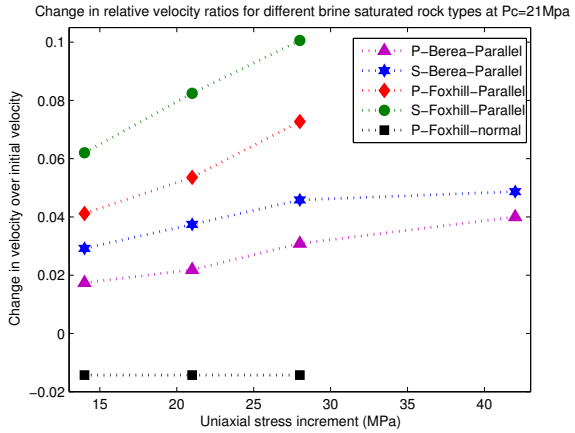

Figure 7: Change in velocities over initial velocity are plotted against change in uniaxial stress. There is velocity increase in the direction parallel to uniaxial stress due to crack closure and it increases with uniaxial stress. There is velocity decrease due to elongation in the direction normal to the uniaxial stress, but the decrease is almost constant.

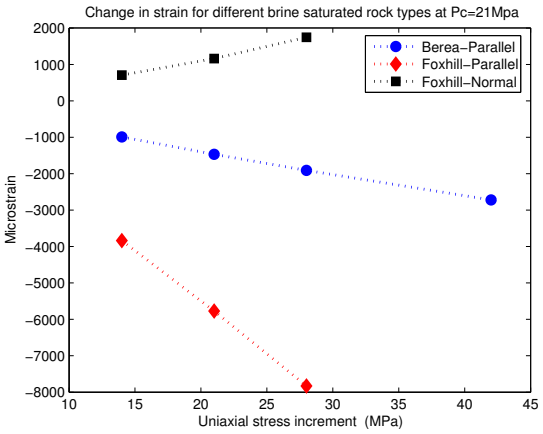

Figure 8: Change in strain with uniaxial stress increments are presented. Strains parallel to the uniaxial stress direction are compaction (negative strain) and increase with uniaxial stress. There is elongation in the direction normal to uniaxial stress direction in Foxhill sandstone. Elongation also increases with uniaxial stress.

can be used to predict reservoir compaction or overburden rise from 4D seismic data, as layer thickness changes cause changes in travel-times and hence seismic velocities.

Janssen et al. (2006) presented a comparison of the R values calculated from 4D seismic data, velocity porosity trends and core analysis. Their core experiments from the Ekofisk reservoir, which is mostly chalk, also show much larger stress sensitivity, than what is observed in seismic data or is predicted from rock physics trends (-R = 10-30). This major contradiction has yet to be explained.

Since R values in sandstones are strongly dependent on the stress states, using a constant value of R at the seafloor (unconfined stress state) and at reservoir depth (higher confined stress state) is an over-simplification. R values are different for P and S waves, especially in the presence of fluids. As PS converted waves are used in 4D monitoring, using the same value of R for P and S waves is another approximation.

Deformation mechanism (dynamic versus static) differences between theoretical models and 4D seismic data should be considered when making any comparison. R values in sandstones are dependent on the mechanisms used to cause the strain.

4D seismic data sees the combined effect of the overburden and reservoir rocks. Hence, in order to compare core analysis results with 4D seismic data, we need to perform similar experiments on samples from the overburden (i.e. shales). The trends in dilation factors with clay content is a critical area to study as most of the overburden rock is composed of shales. Recent analyses of time-lapse data indicate that R value will be higher in shales than in sandstones (Hatchell and Bourne, 2005b; Janssen et al., 2006).

CONCLUSIONS

Our study offers valuable insights into the behavior of R values with respect to stress, deformation mechanism and fluid saturation.

R values in sandstones are strongly dependent on the stress states, hence using a constant value of R from the seafloor to the reservoir depth should be avoided. It is necessary to use the relationships derived from triaxial experiments as these approximate the in situ conditions better. Reduced stress sensitivities of velocities at higher confining pressures and greater strains lead to lower absolute values of R. R values are different for P and S waves, especially in the presence of fluids. Intrinsic anisotropy and stress-induced crack anisotropy play an important role in the understanding of R values, though crack-induced anisotropy is lower at higher confining pressures and in fluid-filled rocks.

Dynamic Young's modulus is generally higher than static Young's moduli as they correspond to different deformation mechanisms. For high aspect ratio pore-dominated rocks, the ratio of dynamic to static Young's modulus remains constant with increasing uniaxial stress. In rocks with a higher density of cracks parallel to the uniaxial stress direction, this ratio increases with uniaxial stress increments. R values in sandstones are dependent on the deformation mechanisms used to cause the strain.

ACKNOWLEDGMENTS

We would like to acknowledge Bob Kranz for many useful insights. We appreciate the help from Matthew Wisniewski in the laboratory. We would like to thank Manika Prasad, Ilya Tsvankin, Luis Tenorio, Ning Lu and Richard Wendlandt for their feedback and discussions. We acknowledge all the members of the Fluid and DHI consortia for the financial support.

EDITED REFERENCES

Note: This reference list is a copy-edited version of the reference list submitted by the author. Reference lists for the 2007 SEG Technical Program Expanded Abstracts have been copy edited so that references provided with the online metadata for each paper will achieve a high degree of linking to cited sources that appear on the Web.

REFERENCES

Hatchell, P. J., A. V. D. Beukel, M. M. Molenaar, K. P. Maron, C. J. Kenter, J. G. F. Stammeijer, J. J. V. D. Velde, and C. M. Sayers, 2003, Whole earth 4D: Reservoir monitoring geomechanics: 73rd Annual International Meeting, SEG, Expanded Abstracts, 1330–1333.

Hatchell, P., and S. Bourne, 2005a, Measuring reservoir compaction using time-lapse timeshifts: 75th Annual International Meeting, SEG, Expanded Abstracts, 2500–2503.

———, 2005b, Rocks under strain: Strain-induced time-lapse time shifts are observed for depleting reservoirs: The Leading Edge, 24, 1222–1225.

Holt, R., O. M. Nes, and E. Fjaer, 2005, In situ stress dependence of wave velocities in reservoir and overburden rocks: The Leading Edge, 24, 1269–1274.

Janssen, A., B. Smith, and G. Byerley, 2006, Measuring velocity sensitivity to production-induced strain at the ekofisk field using timelapse time-shifts and compaction logs: 76th Annual International Meeting, SEG, Expanded Abstracts, 3200–3204.

Jizba, D., G. Mavko, and A. Nur, 1990, Static and dynamic moduli of tight gas sandstone: 60th Annual International Meeting, SEG, Expanded Abstracts, 827–829.

Olsen, C., and I. Fabricius, 2006, Static and dynamic young's modulus of north sea chalk: 76th Annual International Meeting, SEG, Expanded Abstracts, 1918–1922.

Roste, T., A. Stovas, and M. Landro, 2005, Estimation of layer thickness and velocity changes using 4d prestack seismic data: Ph.D. thesis, Norwegian University of Science and Technology.

Sarkar, D., A. Bakulin, and R. Kranz, 2003, Anisotropic inversion of seismic data for stressed media: Theory and a physical modeling study on berea sandstone: Geophysics, 68, 690–704.

Simmons, G., and W. Brace, 1965, Comparison of static and dynamic measurements of compressibility of rocks: Journal of Geophysical Research, 70, 5649–5656.

Thomsen, L., 1986, Weak elastic anisotropy: Geophysics, 51, 1954–1966.

Zimmer, M., 2003, Seismic velocities in unconsolidated sands: Measurements of pressure, sorting and compaction effects: Ph.D. thesis, Stanford University.